Universities of Leeds, Sheffield and York
http://eprints.whiterose.ac.uk/

Nonlinear cellular dynamics of the idealized detonation model: regular cells

G. J. Sharpe†* & J. J. Quirk‡

† School of Mechanical Engineering, University of Leeds, Leeds, LS2 9JT, UK

‡ Los Alamos, New Mexico, NM 87544, USA

High-resolution numerical simulations of cellular detonations are performed using a parallelized adaptive grid solver, in the case where the channel width is very wide. In particular, the nonlinear response of a weakly unstable ZND detonation to two-dimensional perturbations is studied in the context of the idealized one-step chemistry model. For random perturbations, cells appear with a characteristic size in good agreement with that corresponding to the maximum growth rate from a linear stability analysis. However, the cells then grow and equilibrate at a larger size. It is also shown that the linear analysis predicts well the ratio of cell lengths to cell widths of the fully developed cells. The evolutionary dynamics of the growth are nonetheless quite slow, in that the detonation needs to run of the order of 1000 reaction lengths before the final size and equilibrium state is reached. For sinusoidal perturbations, it is found that there is a large band of wavelengths/cell sizes which can propagate over very long distances (∼1000 reaction lengths). By perturbing the fully developed cells of each wavelength, it is found that smaller cells in this range are unstable to symmetry breaking, which again results in cellular growth to a larger final size. However, a range of larger cell sizes appear to be nonlinearly stable. As a result it is found that the final cell size of the model is non-unique, even for such a weakly unstable, regular cell case. Indeed, in the case studied, the equilibrium cell size varies by 100% with different initial conditions. Numerical dependencies of the cellular dynamics are also examined.

1   Introduction

Detonations are supersonic combustion waves which can propagate through reactive materials. In gases, these waves propagate as 'cellular' detonations, where the front is multi-dimensional and time-dependent [1]. If the walls of a shock tube are coated with soot, then, as it propagates down the tube, the detonation etches diamond shaped patterns (known as detonation cells) in the soot (see [2] for a large collection of soot records from different mixtures and initial conditions). In this cellular configuration, transverse shock waves which extend back into the reaction zone intersect the detonation shock front at so-called triple points, dividing the front itself into weaker (incident) and stronger (Mach stem) shock regions. It is the tracks of the triple points, which are regions of high vorticity, that produce the cell patterns in the soot films [1].

The cell patterns in experimental soot traces are loosely classified as either regular or irregular (e.g. [2–5]). In fuel mixtures with regular cells, there is a single characteristic length-scale of the cells, which is highly reproducible between experiments under the same conditions. For irregular mixtures, however, there is range of different length-scales for the cells that appear on the soot trace. For such mixtures, an 'average' cell size may be determined, but there is some ambiguity in defining such a quantity (M. Radulescu, J. Austin, private communications). Nevertheless, the concept of a cell size characteristic to a given mixture (and initial state) is a very useful one, due to several empirical observations of phenomena which appear to scale with this characteristic size. These correlations include the minimum values of (i) the tube diameter in which the detonation can propagate in narrow, smooth walled tubes, (ii) the critical tube diameter for a detonation to survive diffraction out of the end of the tube into open space, (iii) the critical tube diameter for propagation in porous walled tubes, and (iv) the source energy required for the establishment of a detonation from direct (blast) initiation (see [2,4–6] for reviews). The correlations obtained differ between regular and irregular mixtures. For example, in the detonation diffraction problem the critical tube width

*Corresponding author. E-mail: mengjs@leeds.ac.uk

is found to be $\sim 13\lambda$ for regular mixtures, but $\sim 40\lambda$ for irregular mixtures, where λ is the characteristic cell size measured from experimental soot records [4, 5].

Theoretical progress in understanding detonation cells in gases has been achieved by considering the cellular nature of the front to be the result of an instability of the underlying steady, one-dimensional (planar) wave solution. This approach includes linear stability analyses [7–9], weakly non-linear theories [10, 11] and direct numerical simulations [9, 12–17]. Due to the above empirical correlations with cell size, a major objective of theoretical or numerical studies is to predict and understand the dependence of cell size and regularity on the fuel mixture and initial conditions. Much of this work employs a now standard idealized model as defined by Erpenbeck [18], which consists of an ideal gas (polytropic) equation of state, and a one-step chemistry model with Arrhenius kinetics. Numerical simulations using the idealized model have shown that the model appears to contain many of the features observed experimentally, including cells of varying regularity and size, complex transverse wave interactions, and the formation of unburnt pockets of fuel [9, 12–17, 19–21].

However, determining cell sizes from numerical simulations is problematic. Firstly, it has been shown that obtaining detonation dynamics and cell sizes which are grid independent requires high resolution of the detonation reaction zone [16, 17, 22]. Secondly, if the numerical channel width is not sufficiently large, then the computed cell size is determined by the channel width itself, rather than being the natural or preferred cell size of the mixture, due to mode-locking (as is also the case in experiments in narrow tubes [2]). Thus if one is interested in determining the 'natural' cell size, a channel width many times larger than this size is needed to ensure the result is independent of the channel width. However, the characteristic cell size is typically an order of magnitude larger than the one-dimensional detonation reaction zone length. Thus the numerical domain width needs to be about two orders of magnitude larger than the reaction zone length. Combined with the fact that high resolution of the reaction zone is required, this makes accurate and reliable calculations of cell sizes computationally very expensive, even for dynamically adaptive mesh refinement codes. Indeed, even for the simple idealized model, calculations of the cellular dynamics have only been performed using either wide channels but low (possibly insufficient) resolution [19] or higher resolution calculations in narrower channels [9, 15, 16, 21]. As discussed above, neither of these are sufficient to provide reliable intrinsic cell sizes without higher resolution, wide channel calculations to compare with. A noteable exception is a case presented in [15], using a domain sufficiently wide such that several cells formed across it, together with moderate resolution. However, it is unclear whether the run time of this calculation was sufficient to ensure that the cellular evolution was not still in a transitory state (see below).

Since resolved, long time calculations in very wide channels have not been performed even in two-dimensions, a number of even more fundamental questions exist about the idealized model itself. For example, one question is whether the concept of a well defined natural or preferred cell size even exists for the idealized model, i.e. for given initial conditions does the cellular dynamics ever reach a final equilibrium state at large enough times? Calculations in moderately wide channels indicate that the cell size can keep changing between larger and smaller values even after very long times [15, 16]. It is unclear whether this is simply due to the constraints on the cellular dynamics from the presence of the walls in narrow channels (i.e. a mode close to the preferred value is not available in these types of channels) [16]. Even if the cell size does reach an equilibrium value in wider channels, does this equilibrium value depend markedly on the initial perturbation? Also, how long does the detonation have to run for to ensure that a truly equilibrium value has been achieved, in other words how slow or fast are the dynamics of cellular evolution? Furthermore, many different numerical schemes have been used to compute cellular detonations with the idealized model [9, 12, 14–16, 19–21]. Hence fundamental numerical question also exist such as whether the cellular dynamics is sensitive to the flavour of the numerical method used.

The purpose of this paper is to begin to examine and understand these issues with the idealized model, by using a parallel and adaptive mesh refinement approach to solve the idealized model in wide channels. In this first paper, we consider a weakly unstable case with highly regular cells, so that it is clear whether a well defined equilibrium cell size exists for the idealized model and how the final cell size depends on initial perturbations, i.e. avoiding the complication of multiple cell length scales as in irregular cell cases. Furthermore, such weakly unstable cases avoid the necessity to use computationally prohibitive resolutions in order to calculate the cellular dynamics correctly. Indeed, for irregular detonation cases, it appears that

very small scales may be important in the real physical propagation mechanisms (e.g. enhanced rates of burning due to turbulent mixing and small-scale wrinkling at the edges of unburned pockets of fuel and at slip lines) [4, 5, 23], and it would be currently unfeasible to capture such scales in a direct numerical simulation.

Here we only consider the two-dimensional case, since our purpose is to examine the properties of the idealized model system, rather than to model a real experiment. Clearly, it is important to thoroughly understand the nonlinear properties of the two-dimensional solutions before moving on to three-dimensions. Furthermore, resolved three-dimensional calculations would be currently very computationally challenging for the reasons outlined above. It is worth noting that two-dimensional (so-called "planar") detonations have been observed in experiments of very regular mixtures in rectangular tubes [1, 24], but are very rare unless the narrower dimension is much smaller than the characteristic cell size, although then the detonation becomes marginal [24]. In most instances, the structure is three-dimensional ("rectangular" detonations) with orthogonal families of transverse waves, producing cell patterns on both sets of walls, which are typically out of phase [24]. However, Strehlow [24] argues that the rectangular cases consists of two independent planar modes, in which case two-dimensional studies are also relevant to these three-dimensional detonations.

Another question one may ask about the idealized model is whether or not the range and types of cellular dynamics it predicts differ from those found from using more realistic, complex chemistry models. It is well known that the idealized model cannot properly describe the heat release structures of some chain-branching mixtures (e.g. [3, 22]). Nevertheless, one-dimensional calculations of pulsating detonations with one-step and more realistic kinetic models [22, 25] in some cases show qualitatively similar dynamics, e.g. limit cycle oscillations with period doubling bifurcations as the wave becomes more unstable (note that one advantage of the one-step model is that more complex models may actually require significantly higher resolution in order to obtain well converged solutions for these types of dynamics [22, 25]). However, as the instability increases, the one-step model appears to have spurious features which are not present for the more realistic models, such as the lack of a well defined one-dimensional detonability limit. Similarly, one can ask whether the idealized model can essentially describe the full complement of experimentally observed cellular dynamics, by suitable choices of the parameters. While, we do not attempt to answer this question directly here, another purpose of the current study is to provide results using the idealized model which can then be compared and contrasted with future studies using more complex models.

In summary, it is to be stressed here that this paper is concerned with preliminary evaluations of the mathematical properties of the idealized model itself, and not with trying to determine the cell size of any real mixtures at this stage. The structure of the paper is as follows: the idealized model is described in §2; the numerical strategy is discussed in §3; the results are given in §4, while §5 contains conclusions and a discussion.

2   The Model

The idealized model [18] consists of a single reaction step with an Arrhenius form of the reaction rate which releases all the heat, together with an ideal gas equation of state. The non-dimensional governing equations are thus:

$$\frac{\partial \rho}{\partial t} + \frac{\partial(\rho u)}{\partial x} + \frac{\partial(\rho v)}{\partial y} = 0, \quad \frac{\partial(\rho u)}{\partial t} + \frac{\partial(p + \rho u^2)}{\partial x} + \frac{\partial(\rho u v)}{\partial y} = 0,$$

$$\frac{\partial(\rho u)}{\partial t} + \frac{\partial(\rho u v)}{\partial x} + \frac{\partial(p + \rho v^2)}{\partial y} = 0, \quad \frac{\partial E}{\partial t} + \frac{\partial(E u + p u)}{\partial x} + \frac{\partial(E v + p v)}{\partial y} = 0,$$
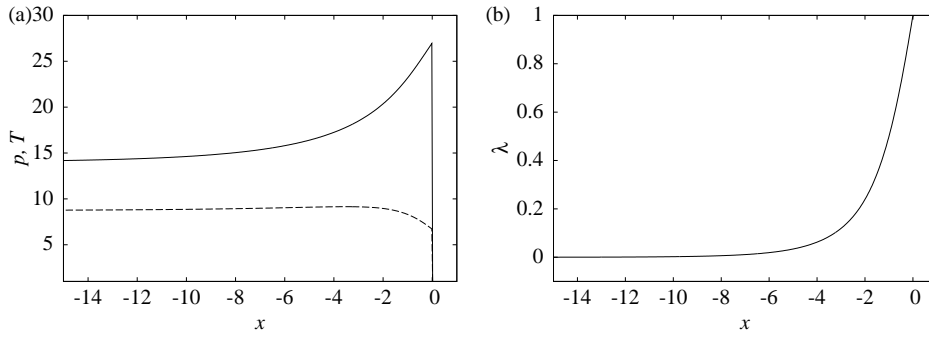
Figure 1.   (a) Pressure (solid line) and temperature (dashed line) and (b) λ profiles for ZND solution when $E_a = 20$, $Q = 11.5$, $\gamma = 1.54$.

$$\frac{\partial(\rho\lambda)}{\partial t} + \frac{\partial(\rho u\lambda)}{\partial x} + \frac{\partial(\rho v\lambda)}{\partial y} = -K\rho\lambda\exp^{(-E_a/T)}, \tag{1}$$

where u and v are the components of the fluid velocity in the x and y directions respectively, ρ the density, p the pressure,

$$E = \frac{p}{\gamma - 1} + \frac{1}{2}\rho u^2 - \rho Q(1 - \lambda),$$

is the total energy per unit volume, λ the reaction progress variable (with $\lambda = 1$ for unburnt and $\lambda = 0$ for burnt), $T = p/\rho$ the temperature, Q the heat of reaction, γ the (constant) ratio of specific heats, E_a the activation temperature, and K a constant rate coefficient.

These equations have been made non-dimensional by choosing the characteristic scales for pressure and density (and hence temperature) to be those in the initial, quiescent (upstream) fuel and K is set such that unit length is the standard half-reaction length, denoted hereafter by $l_{1/2}$ [18]. These equations admit a solution, known as the ZND detonation, in which the wave is steady (in its own rest frame) and one-dimensional. For the self-sustaining (or 'Chapman-Jouguet') detonations of interest here, the idealized model has three adjustable parameters, Q, γ and E_a. In terms of representing a specific mixture, Q and γ can be set, for example, by simultaneously fixing the detonation speed and ratio of temperatures across the shock in the ZND wave to be equal to those found from complex kinetic calculations (e.g. [23]). The activation energy E_a can then be determined via the sensitivity of homogeneous induction times to temperatures near the ZND shock temperature [2, 4, 23]. However E_a also determines the profiles of the ZND heat release structure. As discussed above, the idealized model cannot capture the real reaction zone structure of some fuels. Hence in terms of cellular dynamics, the choice of E_a as a tunable parameter would perhaps be better determined by obtaining agreement with experimental cell records. Again, it is not clear whether the idealized model has sufficient complexity to be able to accomplish this for all fuels.

As we will see, the nonlinear response of the ZND to two-dimensional perturbation is very rich and hence in this first paper we consider a single parameter set in detail. Although we are not attempting to simulate a real fuel in this paper, since we wish to study a weakly unstable, regular cell case, we were guided in our choice of Q and γ by the values obtained for those of a mixture $2H_2+O_2+70\%Ar$, which has extremely regular cells. Fitting the values of Q and γ in the way described above to the results of a detailed chemistry calculation gives $Q = 11.5$, $\gamma = 1.54$ (M. Radulescu, private communication). Note that a large γ has a significant stabilizing effect [8], so this is indeed consistent with a weakly unstable case. The activation energy can then be chosen to enhance the regularity of the cells, since decreasing E_a also has a significant stabilizing effect [7, 8]. Here we use $E_a = 20$. Figure 1 shows the ZND profiles for this parameter set.

For realistic parameters, linear stability analyses show that the ZND wave is always unstable to at least a band of wavelengths of multi-dimensional perturbations of the normal modes form $\exp(\sigma t)\exp(iky)$ [7–9],
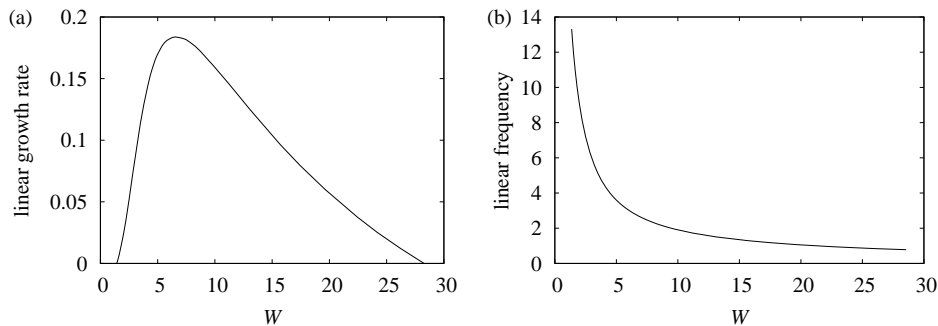
Figure 2. (a) Growth rate and (b) frequency from a linear stability analysis, as functions of the wavelength of perturbation for $E_a = 20$, $Q = 11.5$, $\gamma = 1.54$.

where $k = 2\pi/W$ is the wavenumber of the disturbance in the transverse direction (or wavelength W), $Re(\sigma)$ is the growth rate and $Im(\sigma)$ is the frequency. Figure 2 shows the linear growth rate and frequency versus the wavelength of perturbation for our parameter set, calculated using the method described described in [7]. In this case, there is a single unstable mode, which is unstable to a band of wavelengths between 1.43 and 28.2. The growth rate is maximum for $W = 6.5$, where $Re(\sigma) = 0.184$. However, the maximum in the dispersion relation is rather flat, with wavelengths in the range $6 < W < 7.5$ having growth rates within about 1% of the maximum value. The frequency decreases with increasing wavelength.

3   Numerical method and initial and boundary conditions

In order to perform the simulations with sufficiently high resolution of the reaction zone, but in domains which are much larger than the characteristic reaction zone length scale, we employ a parallelized adaptive mesh refinement strategy [26], within Quirk's Amrita computational environment [27, 28]. The mesh refinement scheme employs a hierarchical system of mesh patches. The coarsest grid, which covers the whole domain, is chosen to have a mesh spacing corresponding to 2 grid points per $l_{1/2}$. Refinement was employed so as to track and resolve the main features of the flow (reaction zones, shocks and slip lines). Unless otherwise specified, the finest grid was chosen so as to give a resolution of 32 points per $l_{1/2}$ in these regions. Resolution studies (see §4.2) showed that this was sufficient to obtain grid independent conclusions and cell sizes for the weakly unstable case considered. A calculation was also performed such that the grid in the entire region behind the reaction zone was kept to a minimum of 8 points per $l_{1/2}$, in order to ensure that the derefinement of the grid behind the reaction zone does not influence the solution. The cellular dynamics/numerical soot trace were unchanged. A numerical scheme based on Roe's linearized Riemann solver was employed using a minmod limiter function [29], although the effect of different choices for the limiter function and solver is investigated in §4.3.

Since we are concerned with intrinsic cell sizes, unless otherwise specified, the domain width was taken to be $240l_{1/2}$. This is a very wide channel as compared to most previous simulations, and is sufficiently wide to be an order of magnitude larger than the characteristic cell sizes. Several of the cases were also ran for a domain width half this size, and one case was re-calculated with a domain of width $480l_{1/2}$ (see §4.1) to ensure that this choice is sufficiently wide that the conclusions are independent of the width. We also use a very long domain (3000 in the x-direction), to ensure that the wave has sufficient time for any initial transients to have decayed before the wave reaches the end of the channel at $x = 3000$. It is important to note that, while in general in §4 we only show parts of the soot record/domain that are pertinent to the discussion, in each case the calculation was always allowed to run until the detonation had reached the end of the domain at $x = 3000$. This is to ensure that an equilibrium configuration has been reached (typically this means that the detonation has propagated for many tens of cell cycles subsequent to the final cell size having been reached). Physical reaction lengths are typically of the order of millimetres to centimetres, so this choice of domain size corresponds to a shock tube of at least 0.24m by 3m. We stress here that our purpose is not simply to perform bigger and better simulations (in terms of domain sizes and numerical resolution) than previous calculations, but it is to perform sufficiently large calculations such

that definite conclusions can for the first time be reached about cell sizes, free from any domain size and resolution dependencies.

The boundary conditions on $y = 0$ and $y = 240$ are symmetry conditions, so that these boundaries represent solid, reflecting walls. The flow state at $x = 0$ is prescribed to be that of the post-detonation (CJ) state, while the boundary at $x = 3000$ is a free-flow (linear extrapolation) conditions.

The initial conditions are given by placing the ZND solution onto the grid, such that the detonation is running left to right in the x-direction as in figure 1, while the initial position of the shock is chosen to be $x = 100$. This is sufficiently far ahead of the rear boundary at $x = 0$ that this boundary does not influence the calculation during the run time, since the post-detonation flow is on average sonic with respect to the front for Chapman-Jouguet detonations. Note the boundary at $x = 3000$ is inactive during the calculation (i.e. while the shock remains in within the domain).

In the simulations, the ZND solution is then perturbed by placing a weak perturbation across the channel just ahead of its initial position. Here we consider two types of perturbation. The first is a weak random perturbation of the form

$$\lambda = 1 - \beta_1 r_1, \quad |x - x_c| \le \beta_2/2 \tag{2}$$

where in each grid cell r_1 takes a random value between zero and one, and the perturbation is applied in a band of width β_2 in the x-direction centred on $x = x_c$. Here we have used $x_c = 108$, and $\beta_1 = 0.1$, and then varied β_2.

The second type of perturbation is of the form

$$\lambda = 1 - \alpha_1 \left(1 - \cos(2\pi y/W)\right) \exp\left(-\alpha_2(x - x_c)^2\right), \tag{3}$$

i.e. a sinusoidal perturbation in the y-direction with wavelength W, and a smooth (Gaussian) perturbation in the x-direction. Here we fix $\alpha_1 = 0.1$, $\alpha_2 = 2$ and $x_c = 108$ (so that the Gaussian is centred at a distance of 8 ahead of the initial shock position), and then study the dependence of the cellular evolution on the perturbation wavelength W. Note that there are only discrete wavelengths compatible with our choice of domain width and boundary conditions, namely $W = 240/n$, $n = 0.5, 1, 1.5, \cdots$, where n corresponds to the number of cells across the channel. The linear stability analysis thus predicts that $n = 37$ is the most unstable mode, with modes $n = 32$ to 40 all having linear growth rates within 1% of the maximum value.

Several methods have been used previously to produce numerical versions of the experimental soot records as a diagnostic for observing the cellular dynamics from simulations. These include recording the maximum pressure reached at each grid point of the numerical domain (e.g. [19–21]), the total heat released at each point (e.g. [16, 30]), or the amplitude of the shock front (e.g. [9, 13]). Since high vorticity at the triple points is believed to be responsible for the etching of the tracks in the experimental soot films, here we have a opted to record the maximum vorticity reached in each grid cell during the calculation [31]. Note that, once the detonation front has passed by, the vorticity record is only stored on the coarsest grid, since the adaptive mesh covers only the front. The vorticity record is plotted on a linear grey-scale in this paper with white corresponding to a value of zero, and black for values of 12 or above, chosen in order to show the cell boundaries clearly.

4   Simulation results

We first consider the response of the ZND detonation to random perturbation of the form (2). All modes are present in such a perturbation, and hence this avoids preferentially stimulating specific wavelengths. We would thus expect that cells will appear with a wavelength (cell width) close to that corresponding to the maximum linear growth rate [16]. The early part of the numerical soot record is displayed in figure 3 for the case $\beta_2 = 4$, which shows that the cells do appear with a characteristic size. Initially, there are about 35 cells across the channel, in good agreement with the linear stability prediction.

Figure 4(a) shows the a numerical schlieren [9,12,14,17,27] picture of part of the detonation front during this initial stage corresponding to a snapshot at $t = 56.60$. The numerical schlieren consists of a linear
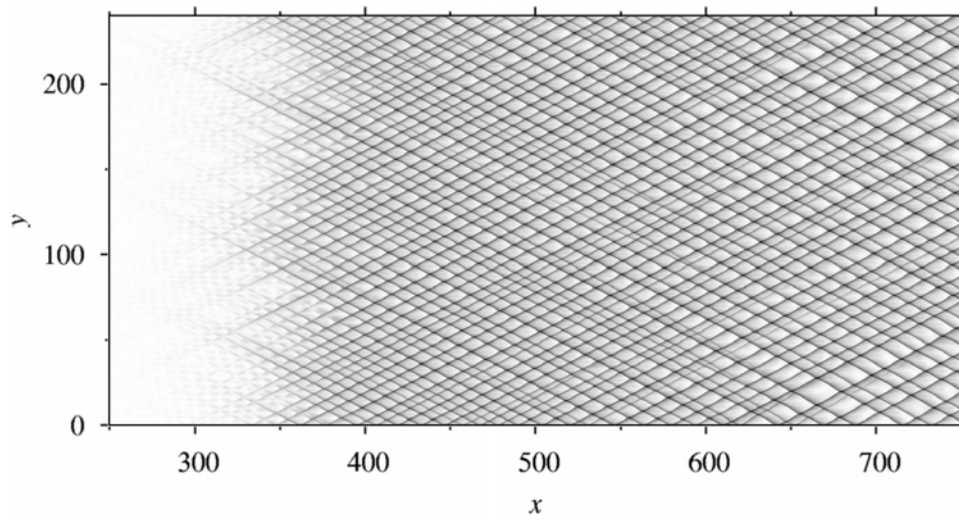
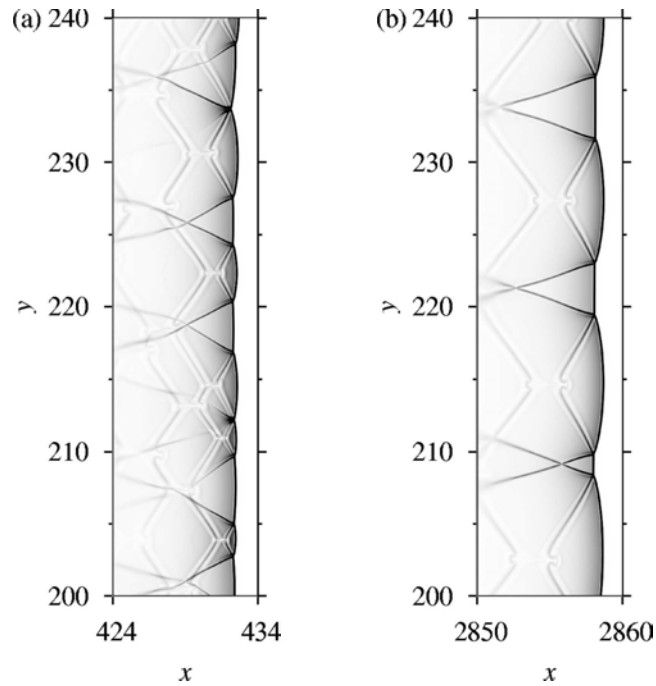Figure 3. Numerical soot record for random perturbation with $\beta_2 = 4$.

Figure 4. Numerical schlierens of part of detonation front within $40l_{1/2}$ from top wall, for random perturbation with $\beta_2 = 4$, at times (a) $t = 56.60$ and (b) $t = 469.26$. Numerical resolution of detonation front is 32 points/$l_{1/2}$.

greyscale plot of the magnitude of the total density gradient,

$$\left[\left(\frac{\partial \rho}{\partial x}\right)^2 + \left(\frac{\partial \rho}{\partial y}\right)^2\right]^{1/2},$$

with white corresponding to zero and black corresponding to a value of 4 or above, chosen so as to best show the main features of the cellular structure (shock front, transverse waves and slip lines separating material which passed through incident shock and Mach stem parts of front). Figure 4(a) shows that at this stage the spacings between transverse waves are non-uniform at a given time, and these waves are also of variable strength. The schlierens are reminiscent of those in [9, 13] for a weakly unstable case with low activation energy, who give a detailed description of this type of observed structure.

However, after the appearance of the cells, figure 3 also shows that the average cell size subsequently

begins to grow as the detonation propagates down the channel (c.f. [16]). The mechanism of the growth is due to the initial transverse waves having different strengths and speeds and some of the original transverse waves then weakening and eventually disappearing, while others strengthen or catch up and merge with the neighbouring transverse wave moving in the same direction.

Figure 5 shows the soot record at subsequent times, in the remainder of the domain. The number of cells across the channel continues to grow initially, but eventually begin to saturate at a constant value of 21 cells across the channel. However, the cells are not all of the same size at this stage. Furthermore, the detonation has to run a considerable distance ($\sim 1500 l_{1/2}$) before the final, equilibrium number of cells is reached. This demonstrates the need for very long time calculations if one is to ensure one has obtained the final cell sizes. Indeed, this run distance is longer than those used in many previous simulations, e.g. [9,15]. If the detonation was only allowed to run for a couple of hundred $l_{1/2}$ say, one would predict a preferred cell size closer to that of the smaller initial cells (as predicted by the linear stability) than to the actual fully nonlinear cell size.

As the detonation continues to run, the cells appear to regulate themselves so that they become of more and more equal sizes across the channel. By the end of the domain, figure 5 shows that the cells have reached a very regular spacing with 21 cells across the domain, i.e. this calculation predicts a preferred or natural cell width of 11.4. Figure 4(b) shows a numerical schlieren when the front is near the end of the channel, at time $t = 469.26$. Note that the transverse waves of different cells are at different points of the cell cycle (out of phase) even at the end of the channel, which results in the cell apexes not lying along a vertical line in the soot trace. The main features of the cellular structure for the fully developed stage are similar to those of the initial cells show in figure 4(a), but on a larger scale.

We repeated the calculation with values of β_2 from 2 to 16 to study whether the cellular dynamics, and the predicted cell size, is sensitive to the initial conditions. In each case, the dynamics were very similar to that shown in figures 3 and 5, in that the cells appear with about 35 cells across the domain, grow and eventually equilibrate to a regular spacing. Very little variation in the final cell sizes was found in these calculations, e.g. for $\beta_2 = 2$, the final cell width is 11.2, or 21.5 cells across the channel, while for $\beta_2 = 8$ the result is again 21 cells.

In order to study the response of the detonation to the initial perturbation further, a series of simulations were performed with the sinusoidal perturbation of the form (3), and various values of the wavelength, W. Figure 6 shows the numerical soot record for the case when $W = 12$ (corresponding to 20 cells across the domain), close to the final cell sizes found from the random perturbation cases above. As expected, 20 cells do appear and then rapidly amplify to saturated nonlinear cells of this size. This structure persists to the end of the channel.

For the random perturbation case, the cells initially appeared with a characteristic size much smaller than the final size. Figure 7 shows the cellular dynamics when the perturbation wavelength is close to the initial value as found in the randomly perturbed cases, i.e. with $W = 8$ corresponding to 30 cells across the domain. Cells of wavelength 8 appear subsequent to the perturbation, again as expected, and amplify until a saturated state is reached. The wave then propagates in this mode of fully developed cells of width 8 for some time. However, after about $900 l_{1/2}$ (or ~ 60 cell lengths), small asymmetries in the cell pattern begin to appear, which are then rapidly amplified. The result is the sudden break down of the initial structure, and growth in the average cell size. The growth is again due to neighbouring transverse waves propagating in the same direction beginning to propagate at different speeds, resulting in the weakening and decay of some of the transverse waves, or merging with the neighbouring waves. The growth saturates at 18.5 cells across the channel, and then regulates into a pattern with cells of width 13 which persist to the end of the channel.

Cells with the initial smaller size ($W = 8$) thus appear to be unstable to symmetry breaking bifurcations, induced here by numerical noise (c.f. [16] who showed that for domain widths small compared to the characteristic cell size, an initial configuration of one cell across the domain will eventually break to form a larger, half cell in the domain). This is confirmed below in §4, where we explicitly perturbed fully developed cells of different wavelengths. Nevertheless, the detonation can sustain the smaller cell size over considerable distances, $O(1000) l_{1/2}$. Again, this is a long run time in terms of many previous simulations, and shows the need for much larger scale calculations if one is to ensure that the correct conclusions about
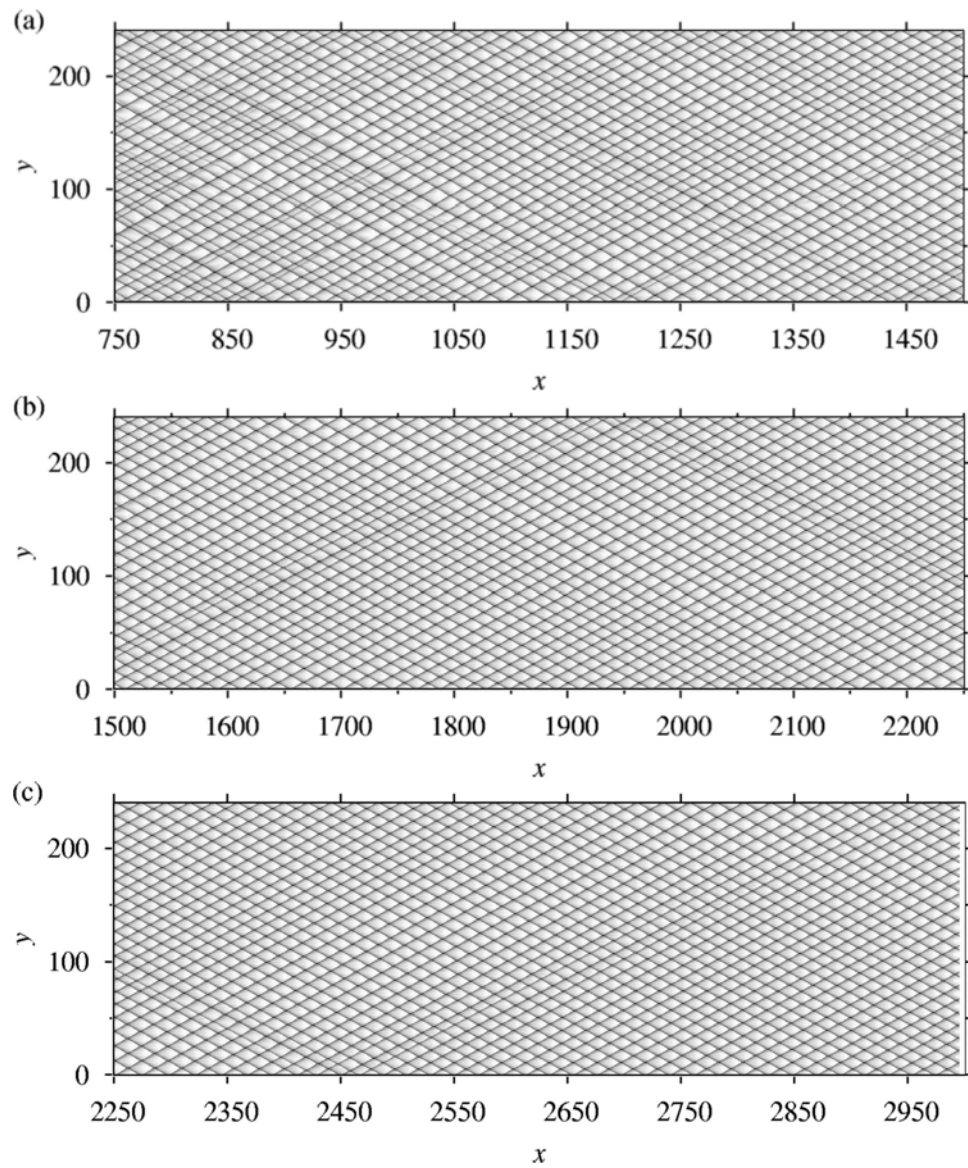
Figure 5. Numerical soot record for random perturbation with $\beta_2 = 4$.
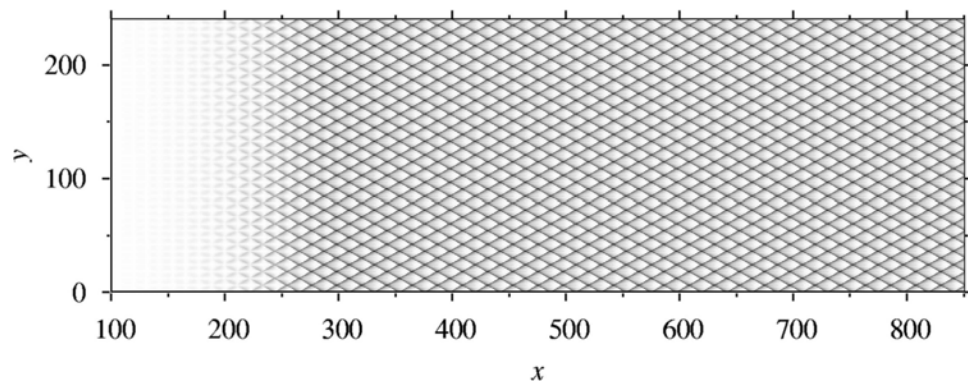

Figure 6. Numerical soot record for sinusoidal perturbation with wavelength $W = 12$ (corresponding to 20 cells across domain).
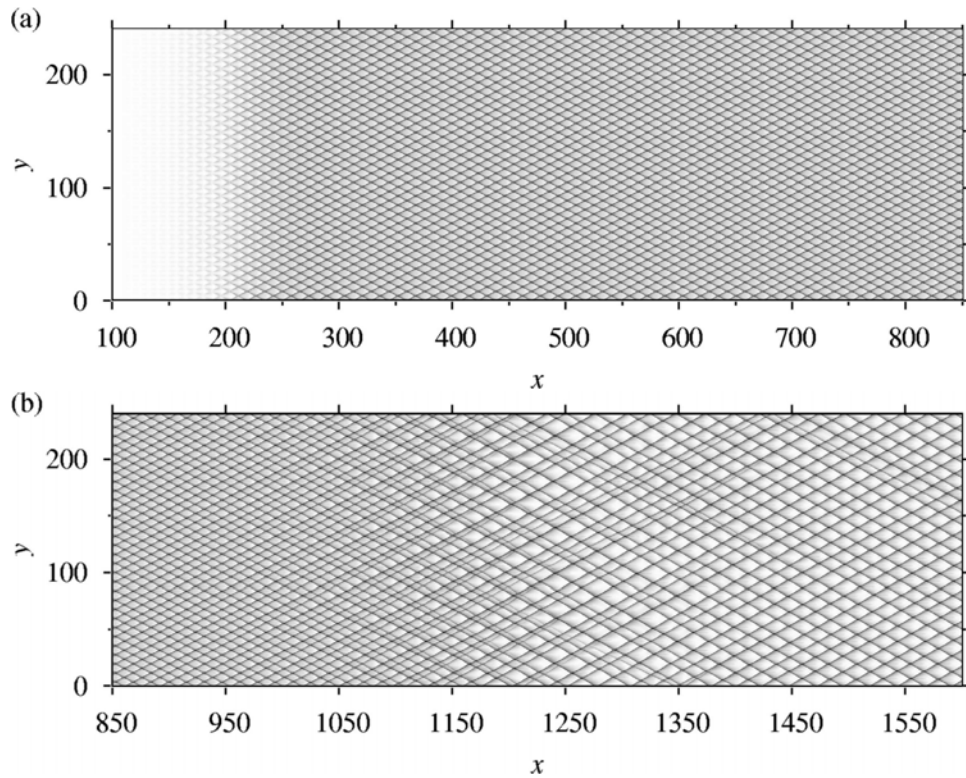
Figure 7. Numerical soot record for sinusoidal perturbation with wavelength $W = 8$ (corresponding to 30 cells across domain).

final or equilibrium cell sizes are reached.

Figure 8 shows part of the numerical soot record for a case with even smaller initial cells corresponding to $W = 4$ or 60 cells across the channel. Again, 60 cells do initially appear and rapidly reach a fully developed nonlinear stage. However, after the detonation has run for about $600l_{1/2}$ (or $\sim$70 cell lengths), asymmetry again begins to creep into the cellular pattern which is rapidly amplified causing growth of the cells. In this case the growth results in the development of a regular structure with 21 cells across, corresponding to a cell width of 11.2. A case with $W = 6$ (40 initial cells) resulted in 20 cells, or a cell width of 12. Note from figures 7 and 8 that as the perturbation wavelength becomes smaller, the transverse waves in the fully developed nonlinear cells corresponding to this size become weaker, as evidenced by the weaker tracks in the soot records for smaller values of W before the initial pattern breaks. It thus appears that the weaker the transverse wave system is, the more unstable it is. By varying W, we found that the smallest wavelength that results in a cellular structure which is sustained to the end of the channel without breaking is $W = 10$ (or 24 cells across the domain). When $W = 9.6$ (25 cells) the initial pattern begins to break after the detonation has propagated about two thirds of the way down the channel (or over 100 cell lengths). The stability of the fully developed cells of different sizes is examined further below.

We now consider what happens when the cell size is increased above that of the range of final cell sizes found above ($\sim 10-12$). Figure 9 shows the early part of the numerical soot traces for the cases $W = 18.5$, 20 and 21.8 (corresponding to 13, 12 and 11 cells across the channel, respectively). In the $W = 18.5$ case (figure 9a), 13 cells do appear and the detonation propagates in this mode all the way to the end of the domain. For $W = 20$, however, while cells of this width do initially begin to form, as the transverse waves strengthen and the cells become nonlinear, a second set of transverse waves also begin to form in the soot record, at around $x = 400$. This second set also strengthen, and initially run parallel and close to their neighbouring counterparts of the primary set of waves. However, they then begin to move towards the centre of the primary cells so that the spacing between all transverse waves moving in the same direction becomes equal. The result is that the initial cells of width $W = 20$ are essentially split into two by the secondary set, thus forming a very regular pattern of cells of width $W = 10$, or 24 cells across the domain. The detonation then propagates in this mode throughout the rest of the channel. Close examination of the $W = 18.5$ soot record also shows that a second set of tracks begin to form at around $x = 400$, but in
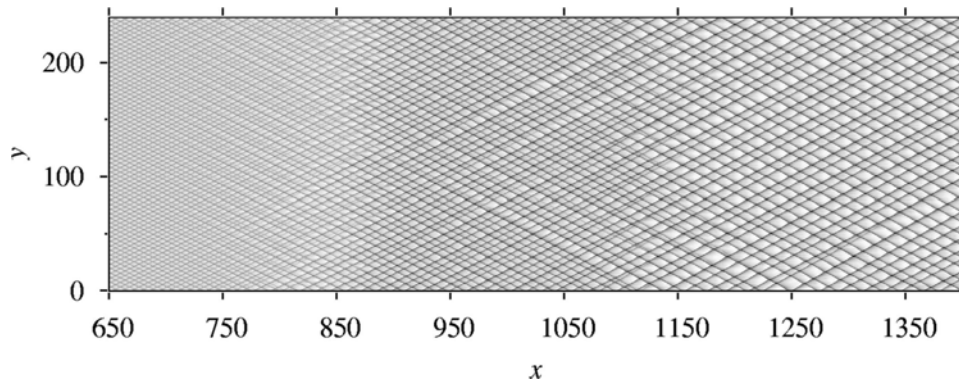
Figure 8. Numerical soot record for sinusoidal perturbation with wavelength $W = 4$ (corresponding to 60 cells across domain).

that case this second set of transverse waves rapidly re-merge with the first set, and hence do not disrupt the initial wavelength.

For larger values of W, the secondary tracks appear when the first set are weaker and with more irregularity, breaking the initial cell spacing earlier (e.g. figure 9c for $W = 21.8$, in which case the final cell size corresponds to 22 cells across the channel, while a case with $W = 24$ results in 21.5 cells). The reason for this secondary wave formation in these larger wavelength cases can be understood from the linear growth rates in figure 2. For larger wavelengths, the growth rate begins to decrease (this can also be seen from figure 9, where the primary tracks take longer to appear and strengthen in the soot trace as W decreases). For example, for $W = 20$ the linear growth rate is 0.055, as compared to the maximum growth rate of 0.184. Thus by the time the secondary tracks appear (after $\sim 300 l_{1/2}$ or a time of ~ 50), the amplitude of the $W = 20$ perturbation would have increased by a factor of ~ 16 during the exponential growth stage. In the same time, modes with closer to the maximum growth would have grown by a factor of $\sim 10^4$. As W increases, so does the disparity in growth rates.

In other words, even very small errors or noise in the system (e.g. truncation errors) can cause smaller wavelength modes to grow and appear before the mode corresponding to the main perturbation wavelength W becomes nonlinear and fully developed (note that even in simulations where no explicit perturbation is given, cells still eventually appear due only to noise [19]). This is confirmed by calculations with increasing amplitude of the perturbation, α_1, which showed that the boundary value of W which actually result in final cells of width W can be (marginally) decreased by increasing α_1. This is due to the primary cells reaching the fully developed stage quicker for larger α_1, before the small wavelengths have time to grow significantly. For example, for $\alpha_1 = 0.4$, a wavelength of $W = 20$ does result in 12 cells at the end of the channel.

The cell width has been used as the measure of the cell size above. An alternative length scale is the cell length. Figure 10 shows the cell length as a function of the cell width for the fully developed cells corresponding to various values of W, as well as the ratio of the length to the width. The ratio decreases slightly as the cell width increases, but is of the order of about two over the entire range. While it hasn't been stated before, the linear analysis also predicts an initial cell length corresponding to each perturbation wavelength. For a given value of W, then the corresponding value of $2\pi/Im(\sigma)$ is the time of one oscillation period (cell cycle) of the front. Hence the distance moved by the front in one period (or the "cell" length) is, to leading order, $2\pi D_{CJ}/Im(\sigma)$, where D_{CJ} is the ZND detonation speed. Figure 10 also shows this linear (or initial) cell length as a function of width W. Interestingly, the linear analysis predicts quite well the cell lengths of the fully nonlinear cells. In other words, the cell length does not vary much with the strength of the cell itself. This is analogous to the fact the linear analysis predicts well the pulsation period of fully developed oscillations in one-dimensional pulsating detonation instabilities, provided one is not too far from the one-dimensional stability boundary, i.e. when the fully developed oscillations correspond to simple limit cycles [22, 25].

The above results show that for weakly unstable cases a range of different wavelengths (cell sizes) can propagate over very long distances ($O(1000)l_{1/2}$, say). For the parameter set considered, this range represents a factor of ~ 5 in the wavelength (from about $W = 4$ to $W = 20$). Moreover, a range of
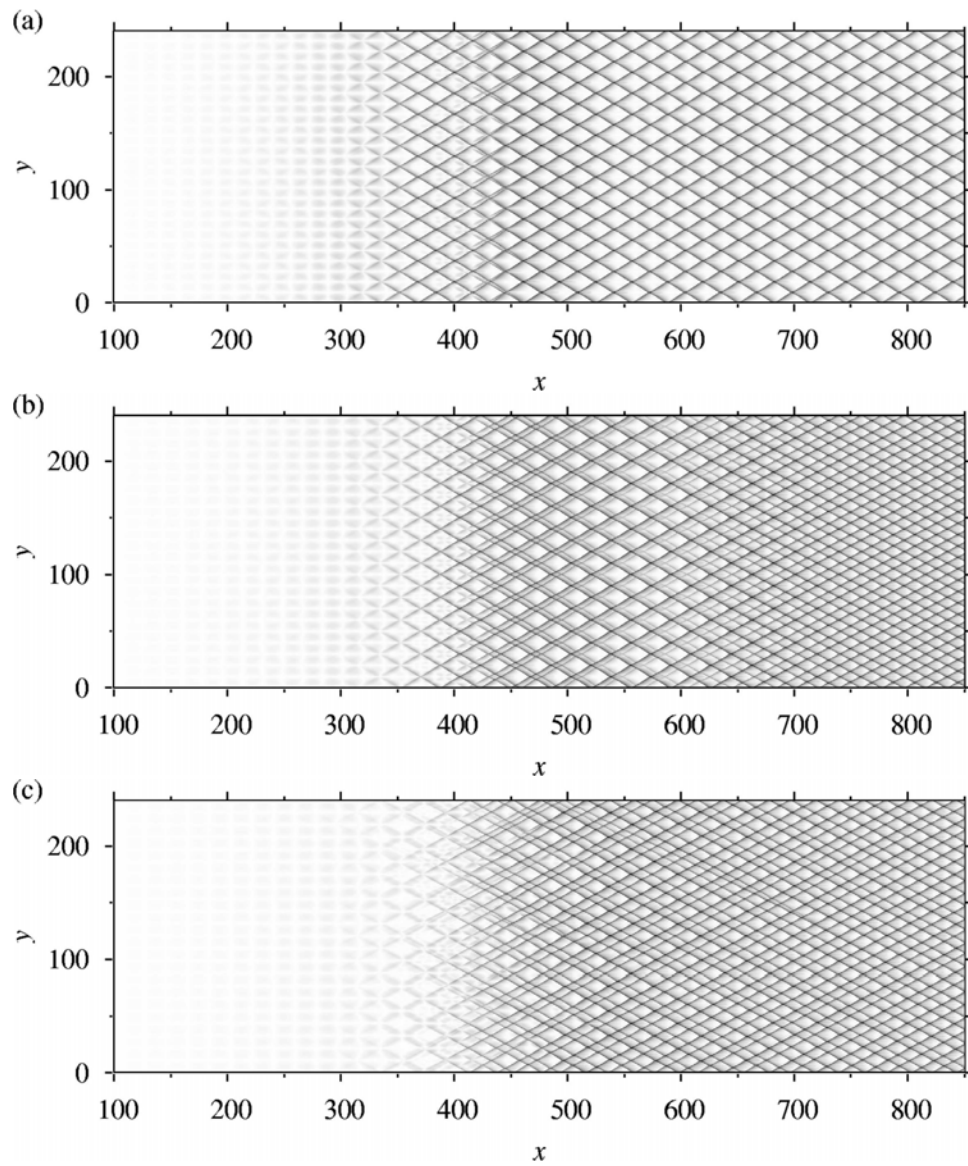
Figure 9. Numerical soot record for sinusoidal perturbation with wavelength (a) $W = 18.5$ (corresponding to 13 cells across domain), (b) $W = 20$ (corresponding to 12 cells across domain), and (c) $W = 21.8$ (corresponding to 11 cells across domain).
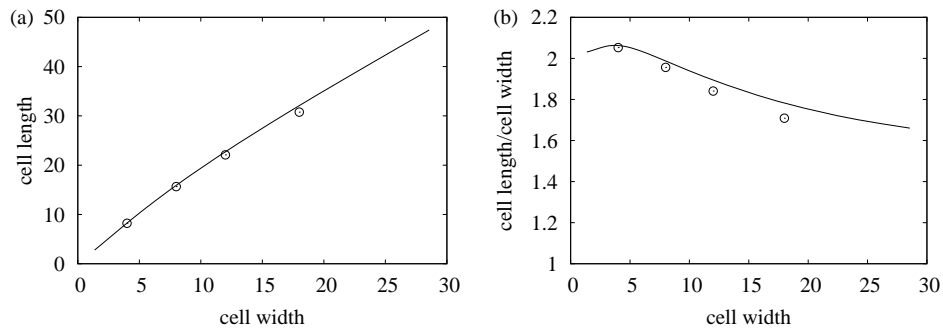

Figure 10. (a) Cell length against cell width, and (b) ratio of length to width, for fully developed nonlinear cells. The solid lines are the predictions of the linear stability analysis, while the circles are data points from numerical simulations.
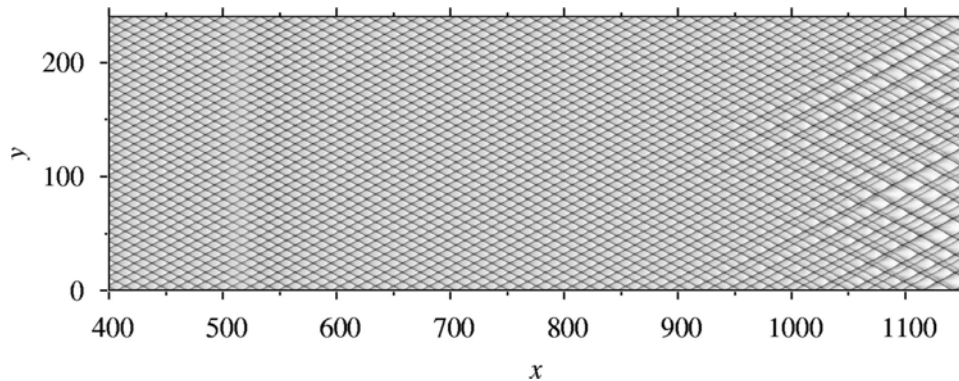
Figure 11. Numerical soot record for sinusoidal perturbation with wavelength $W = 8$ (corresponding to 30 cells across domain), and a second, random perturbation with $x_c = 500$, $\beta_1 = 1$ and $\beta_2 = 10$.

wavelengths from $W = 10$ to $W = 20$, i.e. cell sizes within a factor of 2, propagate for the entire channel length. To examine whether this entire range of cell sizes actually represent stable nonlinear solutions, and to understand why smaller wavelengths eventually break and grow, we perturbed the fully develop cellular structures for the different wavelengths. This was achieved by placing a random perturbation of the form (2) in the region where the cells have become fully developed. Here we chose $x_c = 500$, and use a band width $\beta_2 = 10$. Even for very large amplitude perturbations with $\beta_1 = 1$, it was found that the perturbation had very little effect on the fully developed cells of sizes $W = 10$ to $W = 18.5$ (20 to 13 cells across the domain). The strong transverse wave structure is not disrupted by the perturbation and the wave still continues to propagate in the same mode to the end of the channel. These calculations were repeated in a domain of half the width, $w = 120$, but 6000 long, to determine whether these cell sizes propagated for even longer times. Indeed, for such cases the wave still propagated in the same mode until the end of the longer channel. We also tried a small continual random perturbation with $\beta_1 = 0.01$, on the coarse grid in the entire region of the domain $x > 500$. Again, these modes still propagated to the end of the domain. It thus appears that the nonlinear cells in this entire range are nonlinearly stable. Note that cells larger than this may also be stable, but there appears to be no route to them from the perturbed ZND solution since the corresponding wavelengths have small growth rates.

For smaller wavelengths (for which, when there was no explicit second perturbation, the cell structure broke down and began to grow), the additional random perturbation around $x_c = 500$ causes the cell structure to break down even earlier. For example, figure 11 shows part of the soot trace for the case $W = 8$ (c.f. figure 7). Now the original cell pattern begins to break at around $x = 900$, i.e. $\sim 400 l_{1/2}$, or ~ 25 cell lengths, after the front hit the random perturbation. This shows that cells of width ≤ 9.6 are indeed unstable, and the smaller the cell width, the more unstable the corresponding cellular structure.

Although we found that there exists a band of wavelengths or cell widths which can be induced that appear stable ($20 \geq W \geq 10$), in cases where no specific wavelength is induced, such as in the randomly perturbed cases, or when the original cellular pattern breaks down, as in the short wavelength perturbed cases, the resulting final or equilibrium cell sizes always appear to be towards the lower end of this stable range. Indeed, in all such cases studied, we only found final cell sizes between 10 to 13. This is because the route to the equilibrium solution in these cases is from cells of smaller size (e.g. corresponding to close to the maximum linear growth rate for random perturbations) which *grow* to the equilibrium value. Thus, according to the above, the cells will continue to grow until a stable cell size is reached. The cells will then stabilize at that value and cease to grow. There is of course some variation (30%) in the cell size that the dynamics stabilizes at, as it is dependent on the history of how the transverse waves disappear, but it is unlikely that the larger stable wavelengths will be reached via this pathway.

4.1 *Numerical domain width*

As discussed in §3 and [16], the numerical domain width, w say, limits the degrees of freedom of the solution, in that only cell patterns with a cell width $W = 2w/n$, $n = 1, 2, 3 \ldots$ are compatible with the reflecting boundary conditions, where n is the mode number or number of transverse waves across the
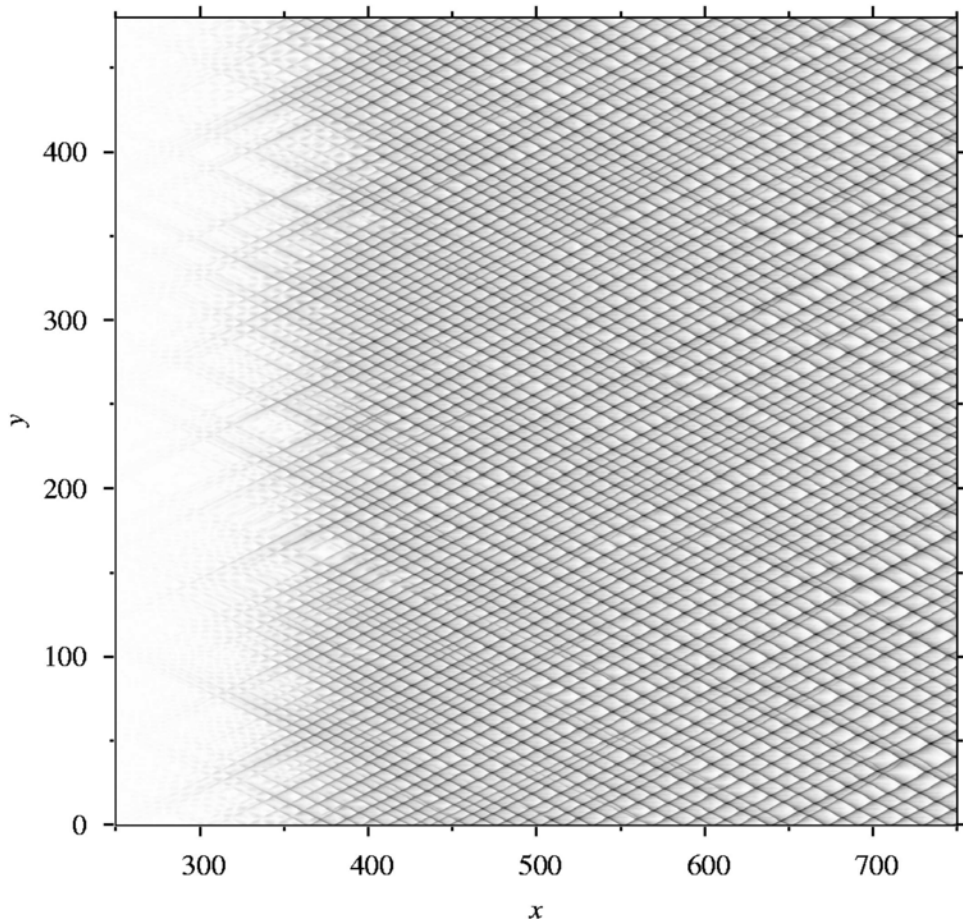
Figure 12. Numerical soot record for random perturbation with $\beta_2 = 4$ in domain of width $480l_{1/2}$.

channel (periodic boundary conditions are more restrictive, with only even modes corresponding to whole numbers of cells, being compatible). The effect of domain width has been examined in narrower domains ($w \sim 3$ to 100) [15], in which case the cell size adjusts to the domain width, but the results in [15] indicate that the cell size is becoming independent of the width as w becomes large compared to the cell size. Indeed, provided w is large compared to any other length scale in the problem (most importantly, the preferred or natural cell size) then one would expect that the boundaries should have little effect on the dynamics, as then there will always be many modes close to the preferred size available for the solution to select.

Nevertheless, it is important to check that the choice of domain size used above, $w = 240l_{1/2}$ (which was chosen such that w is more than an order of magnitude larger than the final cell sizes), is sufficiently large that our conclusions about the cellular dynamics and length scales are indeed independent of w. Figures 12-14 demonstrates this is indeed the case. Figures 12-13 show parts of the soot record for the randomly perturbed case in a wider domain, of width $w = 480l_{1/2}$ (c.f. figures 3 and 5). Firstly, note that the evolutionary dynamics are the same as for the $w = 240l_{1/2}$ case, including the appearance and characteristic size of the initial cells, and the time scale of the growth to the final cell size. Perhaps more importantly, the final cell size reached in the wider domain case, $W = 11.3$ (corresponding to 42.5 cells across this domain), is in good agreement with $W = 11.4$ in the $w = 240l_{1/2}$ domain. Figure 14 shows the soot record in a narrower domain, $w = 120l_{1/2}$, for which the main features of the cellular dynamics are still the same, e.g. the final cell size in this case is again 11.4 (corresponding to 10.5 cells across this domain).
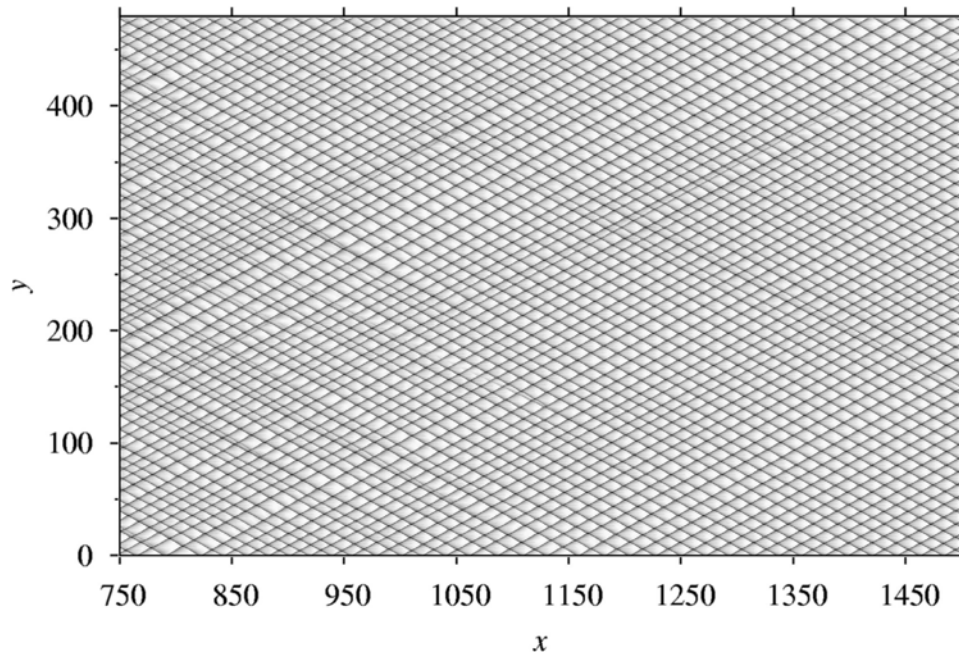
Figure 13. Numerical soot record for random perturbation with $\beta_2 = 4$ in domain of width $480l_{1/2}$.
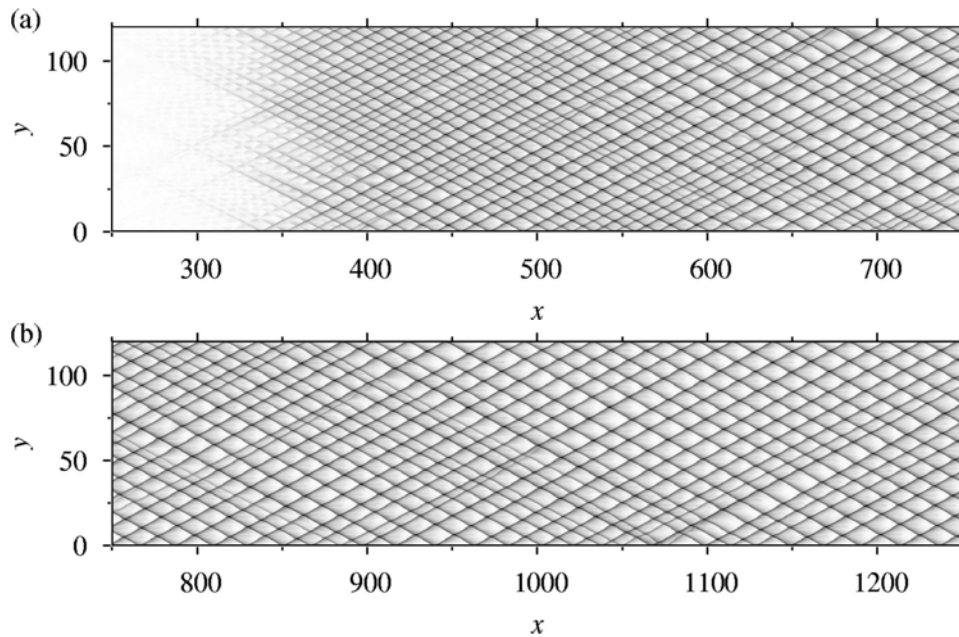

Figure 14. Numerical soot record for random perturbation with $\beta_2 = 4$ in a domain of width $120l_{1/2}$.

4.2   *Numerical resolution*

Previous studies of the idealized and more complex models have shown that the numerical resolution can be an issue with one- and two-dimensional nonlinear dynamics of detonations, and that many tens of points/$l_{1/2}$ may be required to obtain well converged solutions [16, 17, 22, 25]. This is due to the fact that for temperature sensitive Arrhenius kinetics, the reaction zone may change by orders of magnitude during a cell cycle due to oscillations in the shock temperature, and hence very small scale (on the ZND reaction zone length), very transient structures may be involved in the nonlinear instabilities [16, 17, 22, 23, 25], which need to be resolved. Under-resolution may for example result in a large amount of the burning occurring within the numerically smeared shock fronts. Weakly unstable cases, as studied here, typically have reaction rates which are not highly temperature sensitive, and hence the reaction lengths will not
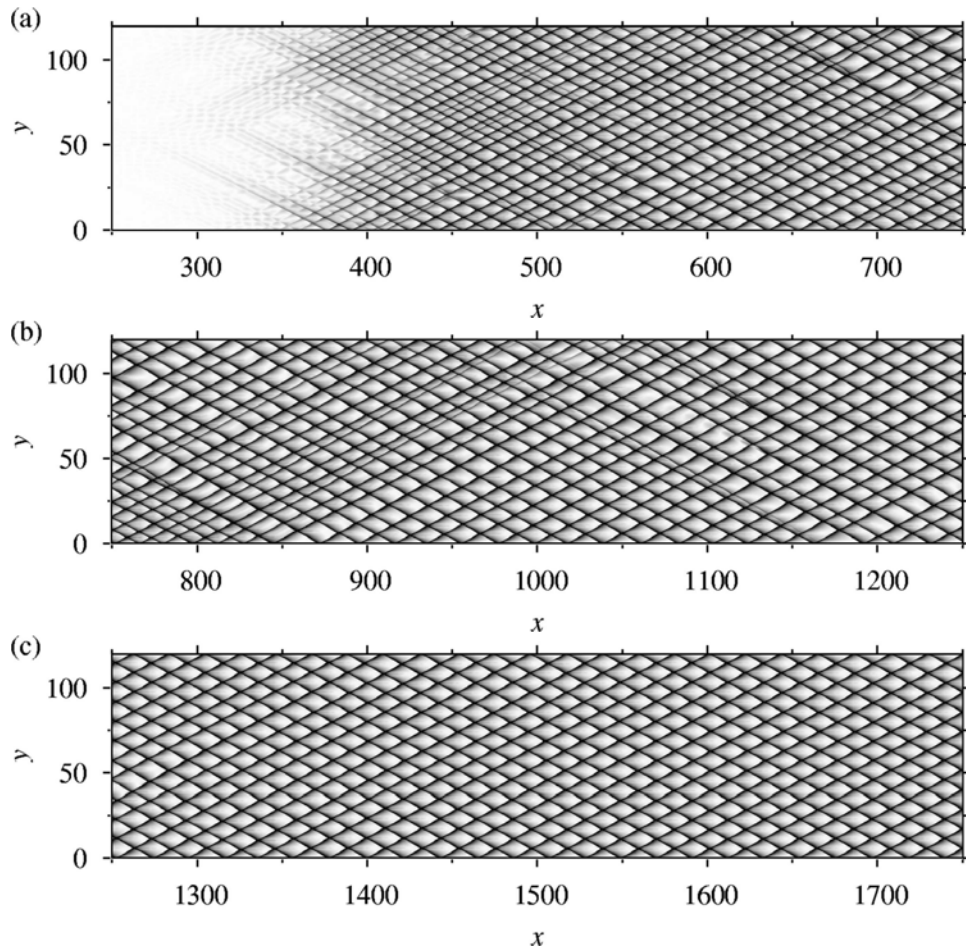
Figure 15.   Numerical soot record for random perturbation with $\beta_2 = 4$ in a domain of width $120l_{1/2}$ and a numerical resolution of 64 points/$l_{1/2}$.

vary too dramatically during a cell cycle. Nevertheless, previous studies show that it is always important to perform resolution studies for any parameter set to ensure that the dynamics (e.g. cell sizes) are grid-independent.

As a first test, we examined the cell length as a function of resolution for fully developed cells of various widths, W (this is akin to using the period of pulsation as a measure of convergence for one-dimensional detonation instabilities [22, 25]. The cell lengths were found to be well converged at our resolution of 32 points/$l_{1/2}$. For example, for a fully developed cell of width 12, the cell length is found to be 22.15, 22.09 and 22.07 for 16, 32 and 64 points/$l_{1/2}$, respectively.

Figure 15 shows the cellular evolution for a resolution of 64 points/$l_{1/2}$ in a channel of width $120/l_{1/2}$, using the random perturbation (c.f. figures 3, 5 and 14). Apart from the tracks in the soot record being stronger for the higher resolution, figure 15 shows that the conclusions about the cellular dynamics are unchanged with resolution. In particular the characteristic initial and final cell sizes are in good agreement with the 32 points/$l_{1/2}$ case shown in figure 14, as are the mechanisms of the growth from the initial (linear) cell size to the final, fully developed non-linear size.

Thus, for the case studied, the resolution of 32 points/$l_{1/2}$ is found to be sufficient for the conclusions about the cellular dynamics and sizes to be grid independent. However, it should not be concluded from this that this level of resolution is sufficient in all cases. Indeed, for more unstable detonations, higher resolutions are likely to be required [17, 22, 25]. Furthermore, as mentioned in §1, for irregular detonations, very small (turbulent) scales appear to be important in the propagation mechanisms, and hence extremely high resolution may be required. In fact, simulations of the Euler equations, where the diffusion is entirely numerical (and grid dependent) in nature, may be inappropriate for such cases [23].
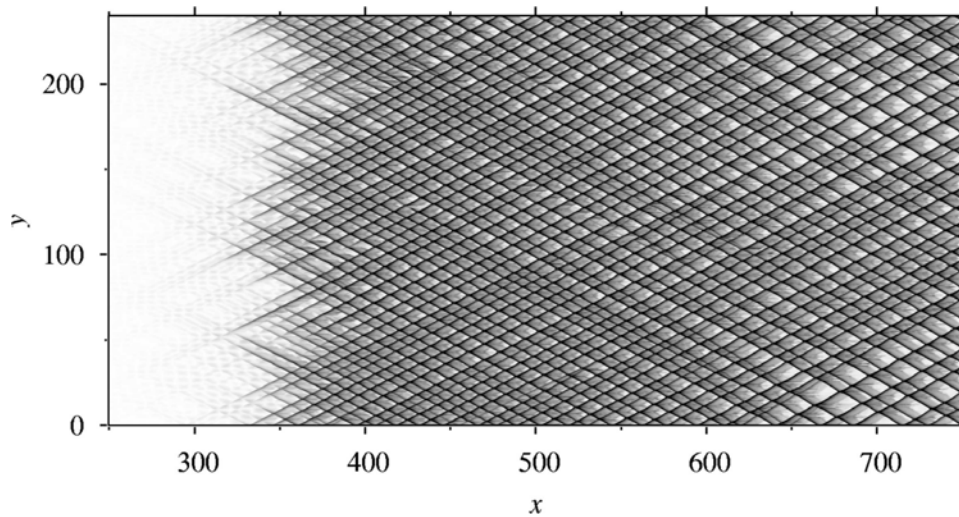
Figure 16. Numerical soot record for random perturbation with $\beta_2 = 4$, using Roe solver with superbee flux limiter.

4.3   Numerical schemes

As well as using different levels of resolution, previous works have all used very different numerical methods to simulate cellular detonation solutions of the idealized model. These schemes will all have different strengths and weaknesses within different parameter regimes [12, 32], and properties such as numerical diffusivities will vary from scheme to scheme. For example, these differences will affect whether sharp features of the flow, such as the slip lines which emanate from the triple points, tend to be diffused or steepened. It is important to consider whether the large scale cellular dynamics are sensitive to the choice of numerical method. If so, then some consensus would have to be reached about what constitutes the correct solution and method.

Figure 16 shows the initial stages of the evolution for the randomly perturbed case with $\beta_2 = 4$, using the Roe solver but with a superbee flux limiter [29]. This type of limiter tends to steepen features of the flow and keep contacts sharp. The triple point tracks in the numerical soot record are much stronger for this flux limiter, and there is more sub-structure within the cells. Nevertheless figure 16 shows that the cellular evolution is very similar to that for the minmod limiter shown in figure 3. In particular, the initial number of cells is in the mid-thirties, then the cell size subsequently grows and at a similar rate to that for the minmod case. The number of cells eventually saturates at 20.5, or a cell size of 11.7, in good agreement with 11.4 for the solution using minmod (given the above results, one does not expect the final cell sizes to be exactly the same, as it depends on the details of the history of the cellular evolution, which does vary from method to method).

Figure 17 shows the solution for the same problem but using a Lax-Friedrichs based solver with WENO reconstruction [33], a method which tends to be quite diffusive. The tracks in the numerical soot trace are weaker than in the Roe solver solutions, but again the cellular dynamics are very similar, and this method also results in a final cell size of 11.4.

Other features of the cellular dynamics are also found to be qualitatively independent of the method. For example, for sinusoidally perturbed cases, the boundary value of the wavelength which results in fully developed cells of that size lies between 18 and 20 (12 and 13 wavelengths across the channel) in each case.

Hence, for weakly unstable cases, it appears that the cellular dynamics and final cell sizes is not too sensitive to the particular numerical scheme. However, this may not be the case for irregular cellular detonation calculations. In these cases, small scales may be physically relevant to the propagation mechanism. The transverse waves cut off large pockets of unburnt fuel, which burn out in the numerics by a combination of artificial diffusion at the pocket boundaries and small scale wrinkling (and hence increases on surface area) due to numerically induced Kelvin-Helmholtz and Richter-Meshkov instabilities [23]. These numerical features are sensitive to the method, such as whether the slip lines become Kelvin-Helmholtz unstable (c.f. the differences between the solutions of the same problem in [12] and [16]), and may lead to qualitative differences in the large scale cellular dynamics.
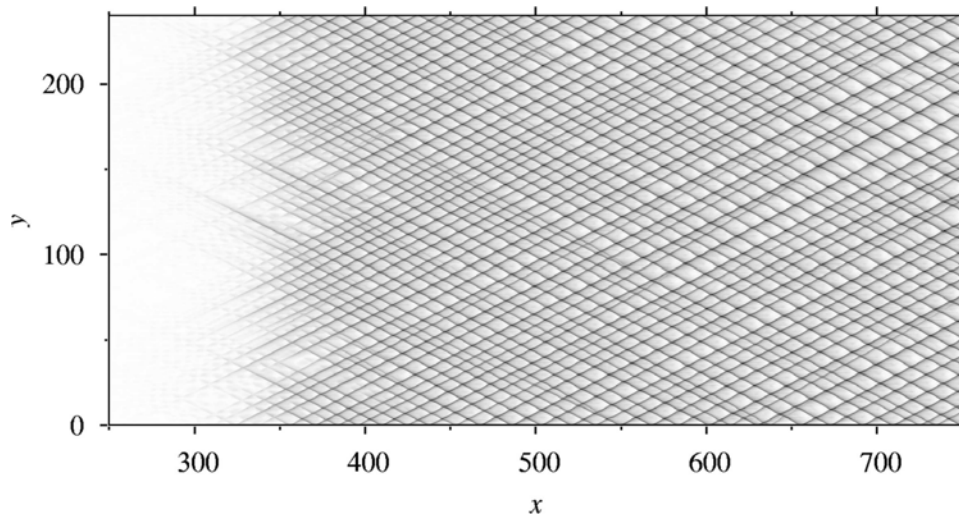
Figure 17. Numerical soot record for random perturbation with $\beta_2 = 4$, using Lax-Friedrichs solver with WENO interpolation.

5   Conclusions

In this paper we have performed a preliminary examination of the cellular dynamics of the idealized detona-
tion model, by considering a weakly unstable (regular cell) case in a wide domain. The main achievement is
the use of a parallelized adaptive grid solver in order to perform simulations which are both high-resolution
and in domains sufficiently wide that the dynamics are not influenced by the boundaries, and sufficiently
long to ensure that a true equilibrium state has been reached. Indeed, we find the dynamics can be quite
slow and hence sufficiently long domains (or long physical run times) are a pre-requisite for ensuring accu-
rate predictions of fully developed cell sizes from numerical simulations. We also find that even for weakly
unstable cases, there is not a unique value of the final cell size reached in the calculations. For the case
studied, when the cells grow from a smaller size, there is about a 30% variation in the equilibrium cell
sizes, while there is a 100% variation in possibly stable, equilibrium cells sizes that can be induced by
discrete perturbation wavelengths.

We also found that, when the ZND wave is randomly perturbed (i.e. no particular wavelength is explicitly
stimulated), the characteristic initial cell size is predicted well by the results of a linear stability analysis.
For these weakly unstable cases, it was also shown that the linear analysis predicts well the ratio of the
cell length to cell width even for the fully non-linear cells.

Numerical dependencies were also examined. At least for the weakly unstable case, it was found that
moderate resolutions (a few tens of points in the reaction zone length scale) were sufficient to provide
grid-independent predictions of cell sizes, and also that the cellular dynamics were not sensitive to the
particular choice of numerical method. However, these factors are likely to become increasingly important
as the detonation becomes more irregular (e.g. as the activation energy is increased).

In a sequel we intend to perform a parametric study to investigate how the predicted cell size (and degree
of variation of the final sizes depending on initial conditions) and regularity vary with the parameters of
the idealized model. We also intend to perform simulations using more complex chemistry models, such as
the three-step chain-branching model used in [22], in order to compare and contrasts with the results of
the idealized model.

6   Acknowledgments

References

[1] Fickett, W. and Davis, W.C. 1979, *Detonation*, University of California Press.
[2] Austin, J.M., 2003, The role of instabilities in gaseous detonation. PhD thesis, California Institute of Technology, California.
[3] Radulescu, M.I. and Lee. J.H.S., 2002, The failure mechanism of gaseous detonations: experiments in porous wall tubes. *Combust. Flame,* **131**, 29–46.
[4] Radulescu, M.I., 2003, The propagation and failure mechanism of gaseous detonations: experiments in porous-walled tubes. PhD thesis, McGill University, Montreal.
[5] Kiyanda, C.B., 2005, Photographic study of the structure of irregular detonation waves. Masters thesis, McGill University, Montreal
[6] Lee, J.H.S., 1984, Dynamic parameters of gaseous detonations. *Ann. Rev. Fluid Mech.,* **16** 311-336.
[7] Sharpe, G.J., 1997, Linear stability of idealized detonations. *Proc. Roy. Soc. Lond.* A, **453**, 2603–2625.
[8] Short, M. and Stewart, D.S., 1998, Cellular detonation stability. Part 1. A normal-mode linear analysis. *J. Fluid Mech.,* **368**, 229–262.
[9] Bourlioux, A. and Majda, A.J., 1992, Theoretical and numerical structure for unstable two-dimensional detonations. *Combust. Flame,* **90**, 211-229.
[10] Stewart, D.S, Aslam, T.D. and Yao, J., 1996, On the evolution of cellular detonation. *Proc. Combust. Inst.,* **26**, 2981–2989.
[11] Clavin, P., 2004, Theory of gaseous detonations. *Chaos,* **14**, 825–838.
[12] Quirk, J.J., 1994, Godunov-type schemes applied to detonation flows. In: J. Buckmaster, T.L. Jackson and A. Kumar (Eds) *Combustion in High-Speed Flows* (Dodrecht: Kluwer Academic), pp. 575–596.
[13] Bourlioux, A. and Majda, A.J., 1995, Theoretical and numerical structure of unstable detonations. *Phil. Trans. R. Soc. Lond.* A, **350**, 29-68.
[14] Williams, D.N., Bauwens, L. and Oran, E.S., 1996, A numerical study of the mechanisms of self-reignition in low overdrive detonations, *Shock Waves,* **6**, 93–110.
[15] Nikolic, M., Williams, D.N. and Bauwens, L., 1999, Simulation of detonation cells in wide channels, In: G.D. Roy, S.M. Frolov, K. Kailasanath, N.N. Smirnov, (Eds) *Gaseous and Heterogeneous Detonations: Science to Applications* (Moscow: ENAS Publishers Ltd.), pp. 153–162.
[16] Sharpe, G.J., and Falle, S.A.E.G., 2000, Two-dimensional numerical simulations of idealized detonations, *Proc. Roy. Soc. Lond.* A **456**, 2081–2100.
[17] Sharpe, G.J., 2001, Transverse waves in numerical simulations of cellular detonations, *J. Fluid. Mech.* **447**, 31–51.
[18] Erpenbeck, J.J., 1964, Stability of idealized one-reaction detonations, *Phys. Fluids,* **7**, 684–696.
[19] Gamezo, V.N., Desbordes, D. and Oran E.S, 1999, Formation and evolution of two-dimensional cellular detonations. *Combust. Flame.,* **116**, 154–165.
[20] Gavrikov, A. I., Efimenko, A.A. and Dorofeev, S.B., 2000, A model for the detonation cell prediction from chemical kinetics. *Combust. Flame,* **120**, 19–33.
[21] Gamezo, V.N., Vasil'ev, A.A., Khokhlov, A.M. and Oran E.S, 2000, Fine cellular structures produced by marginal detonations. *Proc. Combust. Inst.,* **28**, 611–617.
[22] Short, M. and Quirk, J.J., 1997, On the nonlinear stability and detonability limit of a detonation wave for a model three-step chain-branching reaction. *J. Fluid Mech.,* **339**, 89–119.
[23] Radulescu, M.I., Sharpe, G.J., Lee, J.H.S., Kiyanda, C.B., Higgins, A.J., Hanson, R.K., 2005, The ignition mechanism in irregular structure gaseous detonations *Proc. Combust. Inst.,* **30**, 1859–1867.
[24] Strehlow, R.A., 1970, Multi-dimensional detonation wave structure. *Astron. Acta,* **15**, 345–357.
[25] Sharpe, G.J. and Falle, S.A.E.G., 2000, Numerical simulations of pulsating detonations: I. Nonlinear stability of steady detonations. *Combust. Theory Model.,* **4**, 557–574.
[26] Quirk, J.J., 1996, A parallel adaptive grid algorithm for computational shock hydrodynamics. *Appl. Num. Math.,* **20**, 427–453.
[27] Quirk, J.J., 1998, Amrita - a computational facility for CFD modelling. In: H. Deconinck (Ed) 29th Computational Fluid Dynamics VKI Lecture Series, von Karmen Institute. ISSN0377-8312. Available online at: www.amrita-cfd.org/cgi-bin/doc/vki (accessed 31 August 2006).
[28] Quirk, J.J., 1998, AMR_sol: design principles and practise. In: H. Deconinck (Ed) 29th Computational Fluid Dynamics VKI Lecture Series, von Karmen Institute. ISSN0377-8312. Available online at: www.amrita-cfd.org/cgi-bin/doc/vki (accessed 31 August 2006).
[29] Laney, C.B., 1998, *Computational Gasdynamics*, Cambridge University Press.
[30] Oran, E.S., Weber, J.W., Stanfiw, E.I., Lefebvre, M.H. and Anderson, J.D., 1998, A numerical study of a two-dimensional H$_2$-O$_2$-Ar detonation using a detailed chemical reaction model. *Combust. Flame,* **113**, 147–163.
[31] Quirk, J.J., 1994, Numerical soot traces: "The writings on the wall". In: M.Y. Hussaini, T.B. Gatski, T.L. Jackson (Eds) *Transition, Turbulence and Combustion* (Dodrecht: Kluwer Academic), pp. 331-338.
[32] Quirk, J.J., 1994, A contribution to the great Riemann solver debate. *Int. J. Num. Meth. Fluids,* **18**, 555–574.
[33] Liu, X.-D., Osher, S. and Chan, T., 1994, Weighted essentially non-oscillatory schemes. *J. Comp. Phys.,* **115**, 200–212.